Journal of Applied Mathematics and Physics, 2026, 14(2), 961-994
https://www.scirp.org/journal/jamp
ISSN Online: 2327-4379
ISSN Print: 2327-4352

The Second Law Extended to Time-Reversal Asymmetric Systems—Thermodynamic Threshold Optimization

George Samuel Levy

Entropic Power, Irvine, California, USA
Email: glevy#entropicpower.com

How to cite this paper: Levy, G.S. (2026) The Second Law Extended to Time-Reversal Asymmetric Systems—Thermodynamic Threshold Optimization. *Journal of Applied Mathematics and Physics*, **14**, 961-994.
https://doi.org/10.4236/jamp.2026.142046

Received: January 12, 2026
Accepted: February 25, 2026
Published: February 28, 2026

Abstract

Time-reversal asymmetric systems are not bound by H-theorems which assume time-reversal symmetry. Yet few experiments have succeeded in showing anomalous effects by time-asymmetric systems because power output is too low to be observable. Successful experiments must require: 1) time asymmetry and 2) matching measures of asymmetry and of symmetry analogously to source load matching prescribed by the Maximum Power Transfer Theorem in electrical engineering. This paper uses a variation of Maxwell's demon, Szilard's pressure demon, to describe the thermodynamic threshold optimization method applied at the interface between macro and micro scales using conjugate quantities including energy and bandwidth (time). Optimization constraints include the first law applied to the whole system and the second law only to time symmetric components. The optimization criteria are power and bandwidth output. A roadmap is provided for designing devices based on other time-reversal symmetric phenomena such as the *ExB* drift, MIM diodes, and asymmetric membranes. A fully optimized demon acting on air molecules at STP can produce 1276 mW/mm^2, (about 1000 times solar irradiance of 1.33 mW/mm^2), and 74.1 KW/mm^3. This enormous power physically limited by input heat flow, is due to massive parallelism of multiple demons, each one in a chamber 17 nm on the side, and each chamber holding a single particle. Such small dimensions may be achievable on semiconductors in which electrical carriers replace gas particles. The proposed extension to the second law limits power output to half the free energy per second produced by time symmetry-breaking processes. An analogy is made with the Holographic Principle.

Keywords

Maxwell's Demon, Thermodynamic Threshold Optimization, H-Theorem,

Time-Reversal Symmetry, *ExB* Thermoelectric Effect, Entropy, Holographic Principle, Black Hole, Maximum Power Transfer Theorem

1. Introduction

Anomalous thermodynamic effects capable of converting heat isothermally to a useful form of energy have been observed by several researchers in rare but significant instances. For example, Levy [1]-[7] shows that the magnetic field is CPT symmetric and through the $E \times B$ drift can produce such an anomalous thermodynamic effect.

Kondo *et al.* [8] develop an organic thermoelectric device, capable of rectifying electrical thermal noise. Their device produces an open-circuit voltage of 384 mV, a short-circuit current density of 1.1 μA/cm^2, and maximum output Pmax of 94 nW/cm^2.

Lee [9]-[11] shows biological organisms capable of producing ATP isothermally, and without any other source of energy than ambient heat.

Sheehan *et al.* [12]-[15] report an anisotropic diffusion through a chemically asymmetric membrane. The resulting concentration difference drives a concentration cell that produces electrical energy with a power density that might exceed 10^7 Watts/m^3.

Nikulov [16] and Gurtovoi *et al.* [17] observe an anomalous DC voltage on an asymmetric microscopic superconducting ring switched between superconducting and normal state by non-equilibrium noises.

Fu and Fu [18] describe potential difference generated between plates isothermally subjected to a magnetic field in a vacuum tube.

The reader may be puzzled. How can such effects be possible given the theoretical conflict with the H-Theorems by Boltzman [19]-[21], Tolman [22], Gibbs [23], and von Neuman [24] [25] and the fluctuation theorem by Evans, Cohen and Moriss [26], Evans and Searles [27] [28], and Crooks [29]?

There is no conflict. All proofs of the H-theorems and fluctuation theorem assume that physics is time-reversal symmetric. In contrast, all anomalous effects mentioned above rely on time-reversal asymmetrical physics such as the magnetic field or diodes. The magnetic field is CPT symmetric as evidenced by the right-hand rule. Diodes derive their asymmetry by coupling a time varying signal to a static spatial asymmetry or non-linearity. In an ordinary diode, the input signal changes the thickness of the depletion zone dynamically, thereby producing a time asymmetry and favoring the passage of carriers in one direction but not in the other.

The reader may still be puzzled. How can such effects be possible given the paucity of experimental evidence in 200 years of thermodynamic experimentation? Why can't an ordinary PN silicon diode *routinely produce anomalous rectification of thermally induced electrical fluctuations*?

Such phenomena are rarely observed because without careful design their time-reversal asymmetry is not "matched" and is overwhelmed by the background symmetric noise to be rectified. For example, in a conventional PN silicon diode:

1) The frequency response is typically 1 MHz. In contrast, the peak power frequency of the thermally induced electrical fluctuations (*i.e.*, the Johnson Nyquist noise) at 300 K is 17 THz, seven orders of magnitude higher than the diode.

2) The built-in potential of a diode defines its non-linearity or "knee". The energy required for carriers to overcome this barrier is about 700 meV. In contrast, at 300 K, the thermally induced Johnson-Nyquist electrical fluctuations can only provide $\frac{1}{2}k_B T = 12.9$ meV along any given axis. This energy is nearly two orders of magnitude lower than that of the built-in barrier.

Obviously, an ordinary diode is enormously mismatched in amplitude and frequency to the thermal noise to be rectified. Therefore, *the issue is not that a diode cannot rectify thermal electrical fluctuations, it is that its output is too low to be observable*. Accordingly, theoretical, and experimental obstacles highlight *two necessary conditions for observable anomalous thermodynamic behavior*:

1) The Asymmetry Condition: The process must be time-reversal asymmetric to fall outside the coverage of the H-theorems (This can be achieved for example with a magnetic field or with a diode).

2) The Matching Condition: The magnitude of this asymmetry must be "*matched*" to the background thermal fluctuations to make the output observable. This is a new idea introduced by Levy [2]-[7] and discussed in detail in this paper.

"Matching *the asymmetry and the symmetry*" needs to be defined quantitatively. It requires equating *measures that characterize the asymmetry to measures that characterize the symmetry*. Obviously, these measures must be in same units e.g., energy or time. For example, measures of a diode's asymmetry are its built-in potential (in electron-volts) and its carriers recovery time (in seconds). Corresponding measures of thermal fluctuations are the energy of the Johnson-Nyquist noise (in electron-volts) at its peak power frequency, and the corresponding period (in seconds) at that frequency.

Rectifying background ambient thermal fluctuations to produce useable energy can be compared to rectifying a signal in a noisy communication system with one important difference: *The fluctuations play two roles: that of the signal to be rectified into a useful DC output, and that of the noise that obscures the signal.*

These two roles present a double-edged sword, beneficial and detrimental: In the role of the signal, thermal fluctuations are beneficial because they provide the energy to be rectified into a usable output. In the role of the noise, they are detrimental because they dominate and mask the asymmetry required for rectification. This optimization process is in fact a Goldilocks dilemma:

1) If the noise fluctuations are too large compared with the asymmetry or non-linearity of the device, (e.g., the curvature of the "diode's knee" is too flat), then fluctuations dominate, and the system behaves classically in a time-symmetric fashion as predicted by the H-theorems, resulting in an unobservable output.

2) If the fluctuations are too small, they do not provide significant thermal energy to be rectified, also resulting in an unobservable output.

As with Goldilocks, a balance must be struck between two extremes to find a "just right" solution. In quantitative terms, the measures of asymmetry should be neither too large nor too small compared to the measures of symmetry. Maximum output is reached and becomes observable when these measures are commensurate in accordance with the Matching Condition. The ratio of the asymmetry measure to the symmetry measure, *i.e.*, the "signal to noise ratio" should be equal to 1. In the diode example, the curvature of the current-voltage knee should be the same as the amplitude of the noise. The device is then said to operate at the "thermodynamic threshold".

This paper uses Maxwell's demon as a vehicle for formalizing this matching technique. For example, the demon may produce no observable anomalous effect if the width of the trap door is too narrow, or if the demon is not fast enough to activate the trapdoor in response to fast-moving particles. Similarly, an ordinary PN silicon diode may have too high a junction resistance (narrow size of trap door), or too low a frequency response (demon's reaction).

The design strategy for the demon presented in this paper apply to other time-reversal asymmetric phenomena include the $E \times B$ thermoelectric effect [2]-[6], and the isothermal magnetostrictive convection [7] and MIM diodes [8].

Time-reversal asymmetric systems can produce anomalous effects because they are not covered by the H-Theorems. From this perspective, they do not "break" the second law, but merely "bypass" it. Converting heat to usable energy isothermally morphs from the impossible task of falsifying a rigorously derived proof, to an engineering problem that merely requires finding appropriate materials and defining appropriate design parameters to match the asymmetry of the device to the symmetry of thermal processes. Accordingly, *thermodynamic threshold optimization* involves:

1) *Defining a physical model* of the process. This model should include all relevant design parameters to be optimized.

2) *Expressing corresponding measures of asymmetry and symmetry* in terms of these parameters.

3) *Equating corresponding measures of symmetry and symmetry* to solve for optimal design parameters.

The paper shows that a fully optimized time-reversal asymmetric system can utilize the free energy generated by the asymmetry with a limitation analogous to the well-known electrical source-load matching as prescribed by the Maximum Power Transfer Theorem (MPTT). At most, only half of the free energy can be converted to output work. The rest, just like in source-load matching, is used up by resistive friction associated with the heat flow required to replenish the converted thermal energy. This limitation is proposed as an extension of the second law to time-reversal asymmetric systems.

Accordingly, this paper is divided as follows:

Section 2 presents a *qualitative* model of the demon.

Section 3 specifies a *quantitative* model that describes the demon at the macro-scale as well as at the micro-scale. This model includes explicit design parameters suitable for the optimization process.

Section 4 describes the thermodynamic threshold optimization method. It focuses on the interface or threshold between the macro and micro scales using conjugate parameters of energy and time. It uses the first law as an equality constraint, the second law as an inequality constraint, and the output power and bandwidth as optimization criteria. To achieve continuous operation, the conventional piston used by the demon is replaced by a turbine. This method is summarized in Table 1 as described in each subsection:

Table 1. Thermodynamic threshold optimization.

Section	Section 4.1	Section 4.2
Optimization scale	Macro-scale	Micro-scale
Optimization units	Energy	Bandwidth
First law equality constraint.	Section 4.1.1. Conservation of energy. Equation (17) $W_{LoadOutput} = Q_{SourceToLoad}$	Section 4.2.1 Conservation of bandwidth Equation (40) $\beta_{LoadOutput} = \beta_{SourceToLoad}$
Second law equality constraint	Section 4.1.2. Maximum use of free energy. Equations (19) and (20) $W_{LoadOutput} \le G_{DemonToLoad}$ $W_{SourceFriction} \le G_{DemonToSource}$	Section 4.2.2 Full use of demon's bandwidth: Equations (42) and (43) $\beta_{SourceToLoad} \le \beta_{DemonToSource}$ $\beta_{SourceToLoad} \le \beta_{Demon} - \beta_{DemonToLoad}$
Matching Power Transfer	Section 4.1.3 Half demon free energy can be converted to work. Equation (26) $W_{LoadOutput} = G_{Demon}/2$	Section 4.2.3 Half demon bandwidth can be output by load. Equation (45) $\beta_{LoadOuput} = \beta_{Demon}/2$

Section 4.1 covers the macro-scale. It includes:

Section 4.1.1 in which the *first law constrains the work output* by the turbine to be exactly equal to the *net* heat drawn from the heat bath.

Section 4.1.2 in which the *second law constrains the work output* by the turbine not to exceed the free energy produced by the demon.

Section 4.1.3 applies linear programming optimization to show that the work output by the turbine is maximized when it is exactly half the free energy produced by the demon.

Section 4.2 covers the micro-scale. It includes:

Section 4.2.1 in which the *first law constrains the output bandwidth* of the turbine to be exactly equal to the bandwidth of the *net* heat drawn from the heat bath.

Section 4.2.2 in which the *second law constrains the output bandwidth* of the turbine not to exceed the bandwidth of the demon (*i.e.*, the inverse of his reaction

time).

Section 4.2.3 applies linear programming optimization to show that the bandwidth of the information output by the turbine is maximized when it is exactly half the bandwidth of the demon.

Section 5 presents numerical results from equations derived in Section 4. A fully optimized demon operating on air molecules at STP can produce about as much power per unit area as 1000 solar irradiances. Maximum power throughput is achieved when multiple demons operate in parallel, with each demon assigned to a single chamber containing a single particle. Fully optimized chambers measuring 17.33 nm on the side produce a power density of 74.1 KW/mm^3. Obviously, this level of output cannot be sustained longer than approximately the mean free time of a gas molecule and a rapid replacement of the thermal energy converted to work.

Section 6 suggests an extension to the second law to cover time-reversal symmetric systems: Their power output is limited to half of the free energy per second made available by the time-reversal asymmetry.

Sections 6.1 describes attempts at exorcising the demon by Brillouin-Landauer-Bennett. They failed because they rely on circular logic by assuming a demon already compliant with the second law.

Section 6.2 points out that not all laws of nature are time-reversal symmetric.

Section 6.3 asserts that thermodynamics should be extended to time asymmetric systems and allow for negentropy production.

Section 6.4 presents an information-theoretic interpretation of thermodynamics in which particle states are described in terms of thermal energy and bandwidth, both treated as conjugate quantities.

Section 6.5 provides a geometrical interpretation of data channels that links channel capacity to channel cross-sectional surface.

Section 6.6 suggests that the Holographic Principle is applicable to the demon operating on an asymmetric surface (the trapdoor) and an asymmetric black hole bounded by its surface horizon.

Given the controversial nature of this topic, some of the following discussions are done at a fundamental, perhaps elementary level, to provide the reader with a clear, rigorous, and unambiguous understanding of the issues involved.

The reader who wishes to avoid the lengthy mathematical derivations can skip directly to Sections 5 and 6 which present the results of this paper.

2. Qualitative Model of Szilard's Demon

In its original version, Maxwell's demon creates a temperature difference between two compartments A and B separated by a trapdoor and filled with gas. The demon opens the door to fast particles going from A to B and to slow particles going from B to A. This paper uses Leo Szilard's simpler version [30] [31]. As shown in **Figure 1**, his demon produces *a pressure difference* by opening the trapdoor to particles moving from A to B and closing it to particles moving from B to A regardless of their speed.

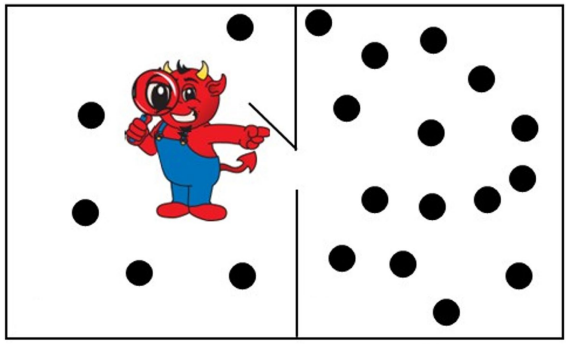

Figure 1. Szilard pressure demon. The demon opens the trap door to particles moving from left to right, thereby creating a pressure difference between the two compartments of the chamber.

This pressure demon is described qualitatively in this section and quantitatively in the next one. Design parameters that need to be optimized can be grouped according to their asymmetry or symmetry.

2.1. Time-Reversal Asymmetric Components

The demon and trapdoor are time-reversal asymmetric. They compress the gas from a low pressure p_1 in A to a high pressure p_2 in B. The door is perfectly elastically reflective when closed and perfectly transmissive when open. Therefore, the energy of the traversing particles does not change. However, their entropy decreases as they are compressed into a smaller volume. This compression is isothermal, adiabatic and negentropic and could be called a "free compression" in analogy to its reverse, the well-known "free expansion". For the sake of analytical simplicity, the customary large swinging trapdoor is replaced by a louvered door or an array of mini trapdoors. Its cross-sectional area is A_{Door}. The reaction time of the demon τ_{Demon} defines how quickly he can observe particles and act on the trapdoor. The negentropy generated by the demon results in free energy G_{Demon} used by the turbine to convert heat to work.

2.2. Time-Reversal Symmetric Elements

The time-reversal symmetric elements include the gas, the chamber, and the turbine.

2.2.1. The Gas and Chamber

The particles behave as an ideal gas according to their pressure p, their concentration n, and their temperature T. The walls of the chamber are perfectly elastic, neither adding energy to, nor subtracting energy from, the bouncing gas particles. The dimensions of the chamber are $\delta_{xChamber}$, $\delta_{yChamber}$, $\delta_{zChamber}$.

2.2.2. The Turbine

For the purpose of achieving continuous operation, a turbine shown in Figure 2, replaces the more customary piston used by Maxwell and Szilard.

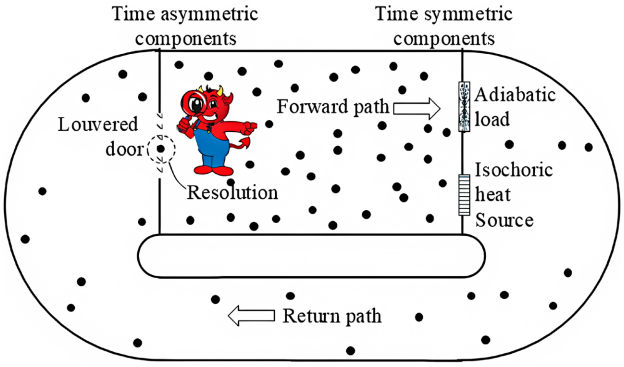

Figure 2. Unoptimized Szilard pressure demon. The demon and turbine are connected in a closed loop. In the forward path, the demon produces an isothermal free compression accompanied by the generation of negentropy and Gibbs free energy which is used in the return path by the turbine (which is composed of an adiabatic load and an isochoric heat exchanger) to achieve isothermal conversion of heat to mechanical energy[1].

The turbine operates at temperature T, drawing heat Q from a heat bath at a higher ambient temperature $T_0 > T$. It converts the energy of the gas $d(pV)$ to mechanical energy dW by transferring particles from the high upstream pressure p_2 to the low downstream pressure p_1. The demon operates isothermally because the trapdoor does not add nor subtract any energy from the gas. Therefore, *the turbine which is connected in a closed loop with the demon must also operate isothermally*. In the context of conventional thermodynamics, an isothermal process is reversible, infinitesimally slow, and *its power output is near zero*. This model is not applicable to this discussion whose goal is to make time asymmetric phenomena observable by *maximizing power production*.

Accordingly, *to make the turbine both isothermal and fast acting*, it is split into two distinct components which operate in tandem in small differential increments: 1) an adiabatic load and 2) an isochoric heat source:

- The "adiabatic load" converts the pressure difference into mechanical energy by expanding the gas particles *adiabatically* without any friction across pressure difference dp, incrementally from p_2 to p_1. As the gas expands, its temperature drops by dT. The cross-sectional area of the load is denoted by A_{Load}.
- The "heat source" functions as an isochoric heat exchanger on the gas, replenishing the thermal energy converted to work by the load and restoring the temperature of the gas from $T - dT$ to T. It operates between the ambient temperature T_0 of the heat bath and the significantly lower output temperature T of the gas. The temperature difference $T_0 - T$ is a Fourier heat flow necessity and not a Carnot efficiency concern which is irrelevant: any heat at ambient T_0

[1]Since the demon causes a free compression, and therefore operates isothermally, under dynamic equilibrium the turbine and heat exchanger in combination must also operate isothermally, independently of how they are connected to each other. They could be connected in series, in parallel, or embedded into each other, the blades and walls of the turbine functioning as heat exchangers. Furthermore, since the demon does not add any internal energy to the gas, the first law requires that in combination, the turbine and heat exchanger must convert the totality of input heat to work with an efficiency of 100%, independently of how "efficiently" the gas expands through the turbine.

entering the turbine and not converted to work is simply returned to the surroundings at T_0. Hence *the work output dW must be exactly equal to the net input heat dQ* implying an overall Carnot efficiency of 100%. The function of the heat source is both beneficial and detrimental. It is beneficial and necessary for continuous isothermal operation. Without thermal energy replenished from the surroundings, the temperature of the gas circulating in a closed loop would drop, and the demon would eventually cease operation. It is detrimental because the very function required for heat exchange, *i.e.*, collisions of particles with the walls of the heat source, results in friction that resists flow, uses up free energy, and lowers the overall power output. This friction is analogous to source resistance in a conventional battery. It leads to the source-load matching approach for power maximization as shall be discussed in Section 4 *Thermodynamic threshold optimization*. The cross-sectional area of the heat source shall be denoted by A_{Source}. *In combination, the adiabatic load and the isochoric heat source constitute the turbine which operates isothermally.*

3. Quantitative Model of the Demon

As explained below, the demon affects the gas at the macroscale and the microscale.

3.1. Operation of the Demon at the Macro-Scale

Szilard's pressure demon decreases the entropy of the gas by transferring particles from a low pressure p_1 to a high pressure p_2. The change in entropy of the gas produced by this transfer is:

$$\Delta S = -Nk_B \ln\left(\frac{p_2}{p_1}\right) \tag{1}$$

Defining an index of asymmetry:

$$\alpha = \frac{p_2}{p_1} \tag{2}$$

Equation (1) becomes:

$$\Delta S = -Nk_B \ln(\alpha) \tag{3}$$

and the corresponding change in Gibbs free energy transferred to the load and heat source is:

$$G_{Demon} = -T\Delta S = Nk_B T \ln(\alpha) \tag{4}$$

3.2. Operation of the Demon at the Micro-Scale

The demon transfers particles through the trapdoor selectively from left to right. Any particle near but not in contact with the door has an equal probability of moving right or left[2]. He opens the door ONLY WHEN APARTICLE ON THE

[2]For the sake of simplicity, the demon and the turbine are assumed to respectively compress and expand a stationary gas. In practice, the flowing gas has a non-zero velocity which results in a decrease in the compression and expansion ratios, and in lower total energy conversion. This velocity-dependent effect is accounted for as a frictional force in the heat source.

LEFT MOVES RIGHT, AND WHEN NO PARTICLE ON THE RIGHT MOVES LEFT. Therefore, the joint probability that a particle traverses the trap door depends on:

- The probability $Pr(L)$ that there IS a particle on the left AND ½ probability that this particle moves from left to right,
- AND
  - The probability $(1 - Pr(R))$ that there is NO particle on the right,
  - OR the probability $Pr(R)$ that there IS a particle on the right, AND ½ probability that it moves from left to right.

Therefore, the transmission probability of a particle through the door can be written as an equation:

$$\begin{aligned} Pr\left(Transmission\right) &= \left[Pr\left(L\right)/2\right]\left[\left(1-Pr\left(R\right)\right)+Pr\left(R\right)/2\right] \\ &= \left[Pr\left(L\right)/2\right]\left[1-Pr\left(R\right)/2\right] \end{aligned} \tag{5}$$

The probabilities $Pr(L)$ and $Pr(R)$ are proportional to the number of particles on either side of the door. Assuming a total of $N_1 + N_2$ particles, with N_1 on the left of the door and N_2 particles on the right, Equation (5) can be rewritten as:

$$Pr\left(Transmission\right) = \left(\frac{N_1/2}{N_1+N_2}\right)\left(1-\frac{N_2/2}{N_1+N_2}\right) = \frac{\left(N_1/2\right)\left(N_1+N_2/2\right)}{\left(N_1+N_2\right)^2} \tag{6}$$

Assuming equal volumes $V_1 = V_2$ on the right and left vicinity of the door in which particles interact with the door, the number of particles can be replaced by their concentration n_1 and n_2 on the left and right respectively, with $n_1 < n_2$:

$$Pr\left(Transmission\right) = \frac{\left(n_1/2\right)\left(n_1+n_2/2\right)}{\left(n_1+n_2\right)^2} = \frac{n_1\left(2n_1+n_2\right)}{4\left(n_1+n_2\right)^2} \tag{7}$$

The flow of particles $\mathrm{d}N/\mathrm{d}t$ is proportional to the probability of transmission, $Pr(Transmission)$, the particle concentration, n_1, the RMS velocity v_{axial} of particles along the X axis, and the area of the door, A_{Door}:

$$\frac{\mathrm{d}N}{\mathrm{d}t} = Pr\left(Transmission\right) n_1 v_{axial} A_{Door} \tag{8}$$

Combining Equations (7) and (8) yields:

$$\frac{\mathrm{d}N}{\mathrm{d}t} = \left[\frac{n_1\left(2n_1+n_2\right)}{4\left(n_1+n_2\right)^2}\right] n_1 v_{axial} A_{Door} \tag{9}$$

Since under isothermal conditions, $\alpha = n_2/n_1 = p_2/p_1$ the particle flow is:

$$\frac{\mathrm{d}N}{\mathrm{d}t} = \left[\frac{2+\alpha}{4\left(1+\alpha\right)^2}\right] n_1 v_{axial} A_{Door} \tag{10}$$

Since $v_{axial} = \mathrm{sqrt}(k_B T/m)$, and $n_1 = p_1/(k_B T)$ (noting that n_1 is a concentration not the number of moles) Equation (10) can be expressed as:

$$\frac{\mathrm{d}N}{\mathrm{d}t} = \left[\frac{2+\alpha}{4\left(1+\alpha\right)^2}\right] p_1 A_{Door} \frac{1}{\sqrt{m k_B T}} \tag{11}$$

and since $n = N/V$, the volumetric flow is:

$$\frac{\mathrm{d}V}{\mathrm{d}t}=\frac{1}{n_1}\frac{\mathrm{d}N}{\mathrm{d}t}=\left[\frac{2+\alpha}{4(1+\alpha)^2}\right]A_{Door}\sqrt{\frac{k_BT}{m}} \tag{12}$$

Combining Equations (3) and (11) yields the rate of change of entropy by the demon on the gas:

$$\frac{\mathrm{d}S}{\mathrm{d}t}=-\left[\frac{2+\alpha}{4(1+\alpha)^2}\ln(\alpha)\right]p_1A_{Door}\sqrt{\frac{k_B}{mT}} \tag{13}$$

Therefore, the free Gibbs power *i.e.*, $\mathrm{d}G_{Demon}/\mathrm{d}t$, available to the turbine (load and heat source) is:

$$\frac{\mathrm{d}G_{Demon}}{\mathrm{d}t}=-\frac{T\mathrm{d}S}{\mathrm{d}t}=\left[\frac{2+\alpha}{4(1+\alpha)^2}\ln(\alpha)\right]p_1A_{Door}\sqrt{\frac{k_BT}{m}} \tag{14}$$

4. Thermodynamic Threshold Optimization

This optimization process has already been applied, albeit in a less formal way, to the $E\times B$ thermoelectric effect by this author [2]-[6]. This method, applied to Szilard's demon is presented as a "roadmap" to be used for other time-reversal asymmetric systems. Table 1 summarizes how salient points of this paper are mapped in this section.

These main points include:

- Optimization is performed at the threshold or interface between macro-scale and micro-scale. At the macroscale, energy and entropy are of concern. At the microscale, information bandwidth and spatial dimensions are applicable.
- Optimization parameters are *conjugate quantities*, energy at the macro-scale and time or bandwidth at the micro-scale.
- Optimization constraints include:
  - The first law applied to the whole system as well as to every component to ensure that the energy budget is balanced everywhere.
  - The second law applied to the turbine (not to the demon) ensures that the work output does not exceed the free energy generated by the demon. It also ensures that the negentropy (information) bandwidth produced by the demon is maximally utilized.
- The optimization criteria include the output power and information bandwidth.
- The optimization method is the thermal analog of the well-known electrical source-load matching as proven by the Maximum Power Transfer Theorem (MPTT).

4.1. Macroscale Optimization in the Energy, Entropy Domain

Optimization at the macro-scale uses the first and second laws as constraints and the power output as the optimization criterion. The optimal flow of free energy, heat and work derived in this section is illustrated in Figure 3. **Appendix 2** describes the thermodynamic cycle of the demon.

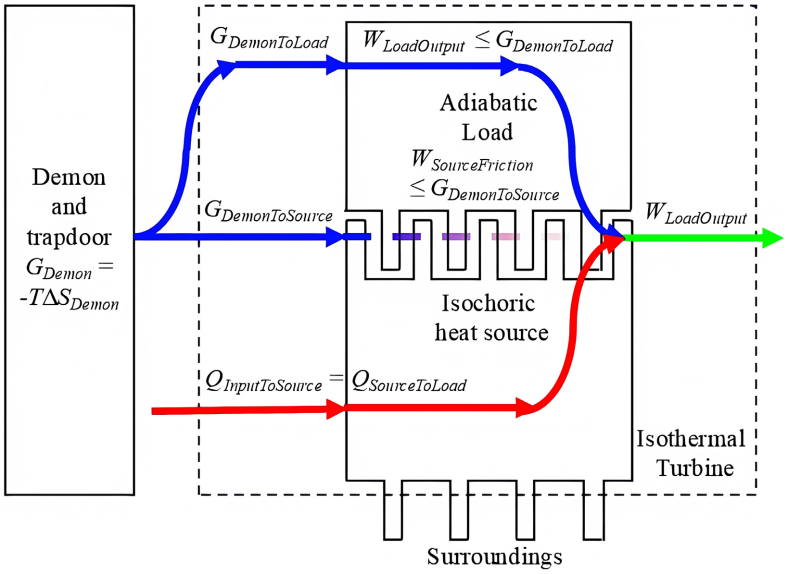

Figure 3. Flow of free energy, heat, and work. The free energy produced by the demon is subjected to the second law inequality constraint as it is divided in the turbine between the adiabatic load and the isochoric heat source. Thermal energy is subjected to the first law equality constraint.

The trapdoor is perfectly transparent to particles moving one way and perfectly elastic to particles going the opposite way. Therefore, it does not add nor subtract energy to the particles. The process through the trapdoor is isothermal and adiabatic ($\Delta U = 0, \Delta Q = 0, \Delta T = 0, \Delta(pV) = 0, \Delta W = 0$). As a result, the gas experiences a free compression in opposition to the well-known "free expansion".

4.1.1. First Law Equality Constraint—Net Heat Input Equals Work

This section discusses the internal energy budget. The free compression produced by the demon *does not contribute any internal energy* to the gas. Therefore, as per the first law, the net energy budget for the components of the turbine which include the load and heat source must be balanced, individually and in combination. The heat source receives a *net amount* of heat $Q_{InputToSource}$ from the heat bath and outputs $Q_{SourceToLoad}$ to the load. Therefore, the energy budget for the heat source is:

$$Q_{SourceToLoad} = Q_{InputToSource} \tag{15}$$

and the load receives $Q_{SourceToLoad}$ which is converted to work $W_{LoadOutput}$:

$$W_{LoadOutput} = Q_{SourceToLoad} \tag{16}$$

Combining Equations (15) and (16) yields the combined energy budget for the turbine:

$$W_{LoadOutput} = Q_{InputToSource} = Q_{SourceToLoad} \tag{17}$$

4.1.2. Second Law Inequality Constraint—Full Use of the Demon's Free Energy

This section discusses limitations imposed by the second law: the work produced

by the turbine cannot exceed the free energy it receives from the demon. Some of the free energy is used up by the adiabatic load to convert heat to work and the rest is diverted by the heat source to account for the frictional loss in the heat exchange process.

This free compression breaks time-reversal symmetry. It generates information which, in the form of negentropy ΔS_{Demon}, results in free energy $G_{Demon} = -T\Delta S_{Demon}$. (Note that ΔS is negative, and G_{Demon} is positive). Some of this free energy, $G_{DemonToLoad}$, is used by the load to produce work and the rest, $G_{DemonToSource}$, is spent in the heat source to overcome friction between the flowing particles and the walls of the heat exchanger.

$$G_{Demon} = G_{DemonToLoad} + G_{DemonToSource} = -T\Delta S_{Demon} \tag{18}$$

The load and heat source are time-reversal symmetric. Therefore, they must comply with the second law which requires that the energy output by the load $W_{LoadOutput}$ cannot exceed the free energy *received* from the demon:

$$W_{LoadOutput} \le G_{DemonToLoad} \tag{19}$$

Similarly, the frictional losses $W_{SourceFriction}$ and the amount of heat $Q_{SourceToLoad}$ transferred from the heat source to the load cannot exceed the free energy $G_{DemonToSource}$ received from the demon. $W_{SourceFriction}$ is converted to the heat $Q_{SourceToLoad}$ transferred to the load.

$$Q_{SourceToLoad} = W_{SourceFriction} \le G_{DemonToSource} = G_{Demon} - G_{DemonToLoad} \tag{20}$$

Equations (18) (19), and (20) express the free energy budget for the turbine. The frictional loss $W_{SourceFriction}$ is due to collisional interaction of particles with the walls of the heat source which operates as a heat exchanger. This interaction is beneficial and necessary as it replenishes the thermal energy converted to work. It is detrimental because it uses up some of the free energy that could be converted to work in the load. This topic, optimizing heat transfer to the load, is discussed in the next section.

4.1.3. Maximum Power Transfer to Load

The Maximum Power Transfer Theorem (MPTT) is well-known in electrical engineering. Power transfer from a source to a load is maximized when the impedance of the source is matched to that of the load, or equivalently when the power dissipated by the source resistance is equal to the power transferred to the load (e.g., battery or resistor). A heat analog of the MPTT shall be derived and used to optimize the operation of the demon.

The optimization criterion is the energy output of the turbine $W_{LoadOutput}$. Three constraints must be considered:

1) An equality constraint required by the first law on energy which includes the input heat $Q_{SourceToLoad}$ required to produce $W_{LoadOutput}$ as shown in Equation (16):

$$W_{LoadOutput} = Q_{SourceToLoad} \tag{21}$$

2) An inequality constraint required by the second law on the free energy transferred from the demon to the load $G_{DemonToLoad}$, which is used to produce $W_{LoadOutput}$

as shown in Equation (19):

$$W_{LoadOutput} \le G_{DemonToLoad} \tag{22}$$

3) An inequality constraint required by the second law on the free energy transferred from the demon to the heat source $G_{DemonToSource}$ which is spent to overcome friction caused by collisions between particles and the wall of the heat source. Since these collisions are necessary for transferring heat from the walls to the gas, $G_{DemonToSource}$ is also commensurate with the heat $Q_{SoureToLoad}$ transferred to the load as per Equation (20):

$$Q_{SourceToLoad} \le G_{Demon} - G_{DemonToLoad} \tag{23}$$

Combining Equations (21) and (23) yields

$$W_{LoadOutput} \le G_{Demon} - G_{DemonToLoad} \tag{24}$$

The work produced by the load can now be expressed in maximin form using Equations (22) and (24):

$$W_{LoadOutput} = \mathrm{Max}\left(\mathrm{Min}\left(G_{DemonToLoad}, \left(G_{Demon} - G_{DemonToLoad}\right)\right)\right) \tag{25}$$

This is a simple linear programming problem solved by replacing the inequalities in Equations (22) and (24) by equalities, and solving the equations. This yields a maximum $W_{LoadOutput}$ when:

$$W_{LoadOutput} = G_{DemonToLoad} = \frac{G_{Demon}}{2} = -\frac{T\Delta S}{2} \tag{26}$$

which is the optimality condition. Figure 4 provides a simple illustration of the conclusions reached in this section.

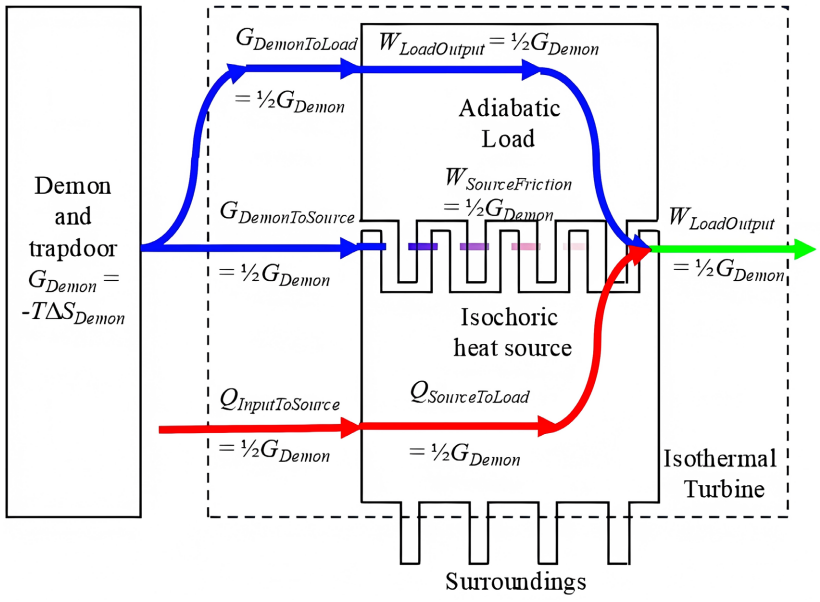

Figure 4. Optimized flow of free energy, heat, and work. The free energy produced by the demon is equally divided in the turbine between the adiabatic load and the isochoric heat source. The maximum power produced by the turbine can only be half of the free energy per second produced by the demon.

Equations (14) and (26) yield power output $P_{Load} = \mathrm{d}W_{LoadOutput}/\mathrm{d}t = ½\ \mathrm{d}G_{Demon}/\mathrm{d}t$:

$$P_{Load} = \left[\frac{2+\alpha}{8(1+\alpha)^2}\ln(\alpha)\right] p_1 A_{Door}\sqrt{\frac{k_B T}{m}} \tag{27}$$

One can show numerically that the term in square brackets reaches its maximum value of 0.042917 for $\alpha = 3.0323$. Hence Equation (27) can be written as:

$$P_{Load} = 0.042917\, p_1 A_{Door}\sqrt{\frac{k_B T}{m}} \tag{28}$$

As indicated in Equation (28), power output increases with the temperature T of the gas. However, T has an upper bound determined by the temperature T_0 of the surroundings. Therefore, maximum power output is obtained by minimizing the difference $T_0 - T$ and maximizing the thermal conductance between the gas and the surroundings.

4.2. Micro-Scale—Time and Bandwidth

The previous section describes an optimization process in which the first law is used as an energy equality constraint, the second law, as a free energy inequality constraint, and the energy output, as the optimization criterion.

This section applies an analogous approach with the same constraints to optimize bandwidth, a quantity conjugate of energy. This analogy is justified by the equivalence between energy and frequency as expressed by Planck's equation $E = hf$. In the physical context, information bandwidth β is essentially the rate of change, or the transmission of entropy $\mathrm{d}S/\mathrm{d}t$. Depending on how it is processed at the microscopic scale, this energy may be conserved as per the first law or, when expressed as entropy, it can be dissipated as per the second law.

The proportionality between bandwidth and energy arises because both scale with the thermal velocity sqrt ($k_B T/m$) and particle flux. The number of information-carrying events per unit time (collisions with the trapdoor) is directly proportional to the energy flux through the same surface. This parallelism justifies treating bandwidth as an effective conjugate variable in the optimization.

Furthermore, in solid-state implementations where electrical carriers replace gas particles, the bandwidth-energy proportionality follows directly from the thermal phonon occupation number, reinforcing the generality of this approach.

The first step is to define the bandwidth of the demon and of the gas particles. This information which is required by the demon to activate the trapdoor for each single particle, changes randomly after each collision. Since collisions occur, on the average, every mean free time, $\tau_{MeanFreeTime}$, the bandwidth required for a single particle is inversely proportional to $\tau_{MeanFreeTime}$. An ideal gas comprised of N particles, each particle having three degrees of freedom, has a bandwidth of:

$$\beta_{Gas} = \frac{3N}{\tau_{MeanFreeTime}} \tag{29}$$

Let the chamber be filled with a Knudsen gas in which particles do not interact with each other, but only collide with the walls of the chamber, the trapdoor, and the turbine. In such a gas, the mean-free-time $\tau_{MeanFreeTime}$ depends only on, and is proportional to, the dimensions of the chamber.

Assuming energy equipartition, then the molecular RMS velocities along the X, Y and Z axes are equal $v_{axial} = v_x = v_y = v_z$. For simplicity, let the mean free times be equal along the X, Y and Z axes by selecting a cubic chamber with dimension:

$$\delta_{Chamber} = \delta_{Chamber,x} = \delta_{Chamber,y} = \delta_{Chamber,z} = v_{axial}\tau_{MeanFreeTime} \tag{30}$$

which implies that the chamber has a cross-sectional area $A_{Chamber} = (\delta_{Chamber})^2$ and volume $A_{Chamber}\delta_{Chamber}$. Since $v_{axial} = \text{sqrt}(k_B T/m)$ Equation (30) can be rewritten as:

$$\delta_{Chamber} = \delta_{Chamber,x} = \delta_{Chamber,y} = \delta_{Chamber,z} = \tau_{MeanFreeTime}\sqrt{\frac{k_B T}{m}} \tag{31}$$

Combining Equations (29) and (31) yields the bandwidth of the gas:

$$\beta_{Gas} = \frac{3N}{\delta_{Chamber}}\sqrt{\frac{k_B T}{m}} \tag{32}$$

Equation (32) is a function of the number of particles but does not represent that the particles are unequally distributed in the chamber. Let the chamber be divided into two compartments of equal volume, with concentrations n_1 and n_2 with $n_2 > n_1$. For a chamber of volume $A_{Chamber}\delta_{Chamber}$, the number of particles is:

$$N = \frac{(n_1 + n_2)}{2} A_{Chamber}\delta_{Chamber} \tag{33}$$

Since the gas is at the same temperature in the two compartments, the index of asymmetry is $\alpha = p_2/p_1$, $= n_2/n_1$ as in Equation (2), Therefore, Equation (33) can be rewritten as:

$$N = \frac{(1+\alpha)}{2} n_1 A_{Chamber}\delta_{Chamber} = \frac{(1+\alpha)}{2} n_1 \delta_{Chamber}^3 \tag{34}$$

The number of particles in Equation (34) can also be expressed in terms of pressure. Since $A_{Chamber} = (\delta_{Chamber})^2$ and $p_1 = n_1 k_B T$ (noting that n_1 is a particle concentration, not a number of moles), yields:

$$N = \frac{(1+\alpha)}{2} \frac{p_1 A_{Chamber}\delta_{Chamber}}{k_B T} = \frac{(1+\alpha)}{2} \frac{p_1 \delta_{Chamber}^3}{k_B T} \tag{35}$$

Combining Equations (32) and (35), yields the bandwidth of N particles of gas, which is proportional to the cross sectional area of the chamber:

$$\beta_{Gas} = \frac{3(1+\alpha)}{2} \frac{p_1 A_{Chamber}}{\sqrt{m k_B T}} \tag{36}$$

The same reasoning can be applied to deriving the bandwidth of the demon and the bandwidth of the turbine. Replacing the cross section of the chamber with the cross section of the trapdoor yields:

$$\beta_{Demon} = \frac{3(1+\alpha)}{2} \frac{p_1 A_{Door}}{\sqrt{mk_B T}} \tag{37}$$

Replacing the cross section of the chamber with the cross section of the turbine yields:

$$\beta_{Turbine} = \frac{3(1+\alpha)}{2} \frac{p_1 A_{Turbine}}{\sqrt{mk_B T}} \tag{38}$$

As in the previous section, the turbine is assumed to comprise two parts, the load, and the heat source. The information (negentropy) bandwidth generated by the demon β_{Demon} is allocated in part to the load and in part to the heat source as shown in Figure 3:

$$\beta_{Demon} = \beta_{DemonToTurbine} = \beta_{DemonToSource} + \beta_{DemonToLoad} \tag{39}$$

4.2.1. First Law Equality Constraint—Conservation of Bandwidth between Load and Heat Source

The information bandwidth output of the turbine can now be maximized using thermodynamic threshold optimization in which the first law is used as an equality constraint and the second law as an inequality constraint. Just like energy, the information bandwidth output by the load must be exactly equal to that which it receives from the heat source:

$$\beta_{LoadOutput} = \beta_{SourceToLoad} \tag{40}$$

4.2.2. Second Law Inequality Constraint—Full Use of Demon's Bandwidth

In accordance with the second law, the information bandwidth output by the load cannot exceed the information bandwidth it receives from the demon:

$$\beta_{LoadOutput} \le \beta_{DemonToLoad} \tag{41}$$

Furthermore, the information bandwidth $\beta_{SourceToLoad}$ sent by the heat source to the load cannot exceed the information bandwidth $\beta_{DemonToSource}$ that the heat source receives from the demon:

$$\beta_{SourceToLoad} \le \beta_{DemonToSource} \tag{42}$$

As per Equation (39) $\beta_{DemonToSource} = \beta_{Demon} - \beta_{DemonToLoad}$. Hence Equation (42) can be written as:

$$\beta_{SourceToLoad} \le \beta_{Demon} - \beta_{DemonToLoad} \tag{43}$$

4.2.3. Maximum Information Transfer to Load

The output bandwidth by the load can now be stated in maximin form using Equations (41), and (43):

$$\beta_{LoadOutput} = \mathrm{Max}\left(\mathrm{Min}\left(\beta_{DemonToLoad}, \left(\beta_{Demon} - \beta_{DemonToLoad}\right)\right)\right) \tag{44}$$

This linear programming problem is solved by replacing the inequalities in Equations (41) and (43) by equalities and solving the equations, yielding the maximum $\beta_{LoadOutput}$:

$$\beta_{LoadOutput} = \beta_{DemonToLoad} = \frac{\beta_{Demon}}{2} \tag{45}$$

This equation matches Equation (26) exactly:

$$W_{LoadOutput} = G_{ToLoad} = \frac{G_{Demon}}{2} \tag{46}$$

Combining Equations (39) and (45) yields the optimal flow of information through the system:

$$\beta_{Demon} = \beta_{DemonToTurbine} = 2\beta_{DemonToSource} = 2\beta_{DemonToLoad} = 2\beta_{LoadOutput} \tag{47}$$

Equations (36), (37), and (38) imply that the optimal cross-sectional area A of the trapdoor, chamber and turbine, should be equal and in the same proportions to their bandwidth β:

$$A = A_{Chamber} = A_{Door} = A_{Turbine} = \beta\left[\frac{2\sqrt{mk_BT}}{3(1+\alpha)p_1}\right] \tag{48}$$

Hence Equation (47) can be written in terms of cross-sectional areas:

$$A_{Door} = A_{Turbine} = 2A_{Source} = 2A_{Load} = A = \delta^2 \tag{49}$$

which indicates that the trap door and the turbine should each occupy a whole wall of the cubic chamber.

The mean-free-path of real gas molecules with diameter d is:

$$\lambda = \frac{k_BT}{\sqrt{2}\pi d^2 p} \tag{50}$$

Setting $\lambda = \delta$, and combining Equation (49) and (50) yields the optimum dimension of the chamber for a real gas:

$$\delta = \frac{k_BT}{\sqrt{2}\pi d^2(1+\alpha)p_1} \tag{51}$$

Equation (26) states that the free energy generated by the demon is twice the energy produced by the load. Equation (49) specifies that the cross sectional areas of the trapdoor should also be twice the cross-sectional area of the load. These two results confirm each other and are illustrated in **Figure 5**.

The results from the previous section can now be combined to obtain the optimal particle concentration, and the dimensions of the chamber, in terms of pressure and temperature. The power to the load and the bandwidth can be shown to be proportional by combining Equations (27) and (48). Since $A_{Door} = A_{Chamber}$,

$$P_{Load} = \left[\frac{2+\alpha}{12(1+\alpha)^3}\ln(\alpha)\right]\beta k_BT \tag{52}$$

This equation describes the power to the load when N particles are assigned to 1 demon, *i.e.*, power to the load can be increased by lowering the number of particles per demon. Maximum power is achieved when a single particle is assigned to a single demon. Accordingly, for a gas with a given mean-free-path λ, the dimensions of the chamber would have to be shrunk to λ.

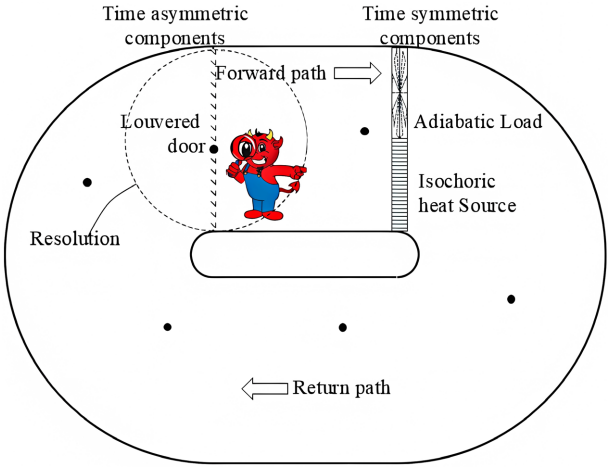

Figure 5. Optimal demon chamber configuration. Design parameters for the demon to be optimized include the dimensions of the trapdoor, load (turbine), source (heat exchanger), chamber, the optical resolution of the demon, and the number of particles in the chamber. In the optimized version, the trap door occupies the whole width of the channel. Furthermore, the load and source equally share the whole width of the channel to maximize power transfer from heat source to load.

$$N = 1 \text{ particle per demon} = 1 \text{ demon per chamber} = 1 \text{ chamber per } \lambda^3 \quad (53)$$

Equation (53) implies an enormous power output due the massive parallelism of multiple demons working within one mean-free-path of each other. Constructing a device at this small scale may be possible with nanoscale semiconductor technology. In solid state, electrical carriers would play the role of gas particles. The $E \times B$ drift, which can compress carriers in a direction perpendicular to the E and B fields would function as the demon. Such an $E \times B$ thermoelectric effect device is described by Levy in [2]-[6].

Figure 6 shows that assigning a single demon to each chamber and a single particle to each demon optimizes data processing of the demon. The multitude of trapdoors and demons in combination tends, in the limit, to acquire a membrane-like architecture with "smart" pores, each pore individually rectifying the flow of gas.

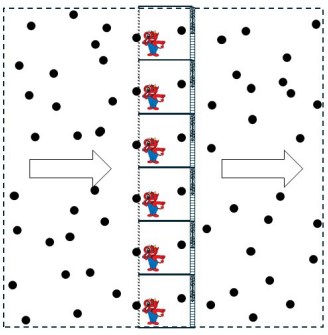

Figure 6. One particle per demon. Optimal data processing performance is achieved when each particle is assigned a single demon, each demon a single chamber, and each chamber is as large as a mean free path.

5. Results

Equation (28) yields the power per unit area. For air molecules at $T = 300$ K, at atmospheric pressure of 101,332 N/m^2 and an average molecular mass of 0.02897 kg/mole/6.022 × 10^{23} molecules/mole = 4.81 × 10^{-26} kg, the maximum power per unit area is:

$$\frac{P_{Load}}{A_{Door}} = 0.042917 \times 101332\ \mathrm{N \cdot m^{-2}} \sqrt{\frac{13.80649 \times 10^{-24}\ \mathrm{m^2 \cdot kg \cdot s^{-2} \cdot K^{-1}} \times 300\ \mathrm{K}}{4.81 \times 10^{-26}\ \mathrm{kg}}} = 1276\ \mathrm{mW/mm^2} \tag{54}$$

This is about 1000 times the solar irradiance of 1.33 mW/mm^2 [32] [33]. This assumes demons capable of reacting within a mean-free-time, at the thermal velocity timescale (~10^{-10} s for air at STP).

Equation (51) can be used to calculate the optimal size of the chamber. For a temperature $T = 300$ K, the average diameter of an air molecule, $d = 0.364$ nm, the atmospheric pressure p_1 = 101,325 N/m^2, and $\alpha = 3.0323$ m, then the size of the cubic chamber is:

$$\delta_{Chamber} = 17.22\ \mathrm{nm} \tag{55}$$

Given a thickness of 17.22 nm, and a power per unit area of 1276 mW/mm^2, the power per unit volume is 74.1 KW/mm^3. As described in Equation (53), this enormous power generated in a volume of 1 mm^3 is due to the large number of demons, all working in parallel, each occupying a tiny chamber and each processing on the average a single particle at a time. Obviously, unless the converted heat is quickly replenished at an extraordinary rate, the demons must stop operating within the mean-free-time of an air molecule of about 0.1 nanoseconds. These calculations represent an upper bound under idealized conditions.

The power output per unit area and the input heat flow scale equally with area. Furthermore, they must be equal to each other in accordance with the first law. Therefore, the limitation in the thermodynamic performance of the demon is better expressed in terms of power per unit area as per Equations (27) and (54), (e.g., 1276 mW/mm^2):

$$\frac{P_{Load}}{A_{Door}} = \left[\frac{2+\alpha}{8(1+\alpha)^2}\ln(\alpha)\right] p_1 \sqrt{\frac{k_B T}{m}} \tag{56}$$

rather than by power per unit volume (e.g., 74.1 KW/mm^3). This surface-caused limitation also applies to the demon as an information-processing system to be further discussed in Sections 6.4-6.6.

6. Discussion—Suggested Extension of Second Law to Include Time-Reversal Symmetric Phenomena

Central to this discussion is the role of time symmetry with respect to the second law. Symmetry implies lower complexity and redundancy of information: in other words, fewer bits are needed to describe a system. A conventional thermodynamic

process is reversible when its time forward and time reverse behaviors are symmetric and determined by exactly the same information (entropy). Redundancy derived from time-reversal symmetry implies that less information is needed to describe behavior in time.

This information redundancy does not apply when time-reversed symmetry is broken by unidirectionally added new states. The information associated with these new states makes reversibility impossible and precludes equilibrium by enforcing a forward or reverse direction. Accordingly, a complete formulation for changes of entropy with time should have two components:

1) A classical component ΔS_A which encodes changes in information associated with the dynamics of time-reversal symmetric "A" processes.

2) An anomalous component which encodes changes in information of anomalous "B" processes that break time-reversal symmetry.

Therefore, the net change in entropy ΔS of a system should be the sum:

$$\Delta S = \Delta S_A + \Delta S_B \tag{57}$$

Furthermore, second law limitations should extend to systems that comply with time-reversal symmetry as well as asymmetry.

Time-reversal symmetric processes. These are conventionally governed by the H-theorem which states that entropy ΔS_A cannot decrease in a closed system:

$$\Delta S_A \geq 0 \tag{58}$$

Time-reversal asymmetric processes. They can generate a negentropy ΔS_B:

$$\Delta S_B \leq 0 \tag{59}$$

and an associated free energy $\Delta G_B = -T\Delta S_B$. However, as shown in Equation (26) the work that can be generated from this free energy is limited and cannot exceed half of ΔG_B.

$$W \leq \frac{\Delta G_B}{2} = -\frac{T\Delta S_B}{2} \tag{60}$$

Equality in Equation (60) is satisfied when the measures of time asymmetry are matched to the measures of time symmetry. The remainder of the free energy is dissipated in converting heat to work. ***This equation explains why most time asymmetric phenomena do not manifest any anomalous effect. Without careful design, the asymmetry and symmetry are not matched, the inequality prevails, and the effect remains too small to be observable.***

6.1. Exorcising of the Demon—Relation to Brillouin-Landauer-Bennett

The anomalous behavior of the demon presented in this paper must be discussed in the context of current literature. Modern "information-theoretic" exorcisms of Maxwell's demon trace back to Brillouin [34] [35], Landauer [36], and Bennett [37] [38]. In different ways, all three work within the standard framework of statistical mechanics, which assumes time-reversal-symmetric microscopic dynamics (Hamiltonian or unitary evolution) and Liouville's theorem for phase-space

volume preservation. Within that setting, they conclude that any demon must pay at least as much entropy (in measurement and/or erasure) as it apparently removes from the working substance [34].

In classical statistical mechanics, the microstate $x=(q,p)$ evolves under a Hamiltonian flow that preserves phase-space volume. The probability density $\rho(x,t)$ obeys the *Liouville equation*:

$$\frac{\mathrm{d}\rho}{\mathrm{d}t}+\{\rho,H\}=0 \tag{61}$$

which is invariant under time-reversal and implies that coarse-grained entropy cannot decrease on average except through probabilistic assumptions over initial conditions. Brillouin explicitly interprets thermodynamic entropy as a measure of missing information about such phase-space distributions and argues that acquiring one bit of information (e.g. by a measurement performed by the demon) must be paid for by at least $k_B\ln 2$ of entropy production elsewhere, leading to his "negentropy principle of information" [35].

Landauer's analysis [36] of logically irreversible operations and Bennett's subsequent reversible-computation treatment of Maxwell's demon [38], also depend on this Liouvillean, time-symmetric behavior. In Landauer's canonical example, compressing an ensemble of memory states halves the accessible phase-space volume; using the **second law for a closed system** ("its thermodynamic entropy cannot decrease"), he infers that the missing $k_B\ln 2$ per bit must reappear as at least $k_B\ln 2$ of heat dumped into the environment [36]. Bennett then embeds information processing in a globally reversible (Hamiltonian or unitary) dynamics and attributes the demon's thermodynamic cost to the logically irreversible step of memory erasure rather than to measurement itself [37].

From the present viewpoint, these arguments all share two key assumptions:

1) Microscopic time-reversal symmetry and Liouville's theorem are applied to the demon.

The demon, its memory, and the gas are ultimately governed by reversible dynamics that preserve phase-space volume (or, in the quantum case, by unitary dynamics on a fixed Hilbert space). All effective irreversibility must be statistical, *arising from coarse-graining or discarding information*, *not from any intrinsic arrow of time* in the underlying equations.

2) A global second-law constraint for closed systems.

The step from phase-space compression to heat dissipation is made by *invoking* the empirical or axiomatic statement that the entropy of a closed system cannot decrease. This is exactly what enforces the inequality "entropy cost of information processing ≥ negentropy gained".

These assumptions set up a strawman demon which leads to the Brillouin-Landauer-Bennett conclusion:

"*The demon must spend at least as much entropy as the negentropy that it generates".*

It is not about *arbitrary* demons, but about demons realizable within a *time-*

reversal-symmetric Liouvillean framework. In the notation of this paper, these analyses effectively set $\Delta S_B = 0$ and consider only the time-symmetric contribution $\Delta S_A \geq 0$.

A strawman demon compliant with the second law is easy to exorcise: any apparent reduction of the gas entropy $\Delta S_A < 0$ must be compensated by at least $-\Delta S_A$ elsewhere in the combined system, typically in the demon's memory or its heat bath.

By contrast, the present work explicitly considers the possibility of a *time-reversal-asymmetric demon*, for which $\Delta S_B < 0$ is allowed and the microscopic dynamics need not preserve phase-space volume in the Liouvillean sense. For such a demon, the standard derivations are no longer relevant:

- If the effective dynamics in the demon's channel are not time-reversal symmetric, Liouville's theorem does not apply in the usual way to that channel, and volume-preservation arguments cannot be used to constrain its entropy balance.
- If the global second-law constraint is *assumed* in order to re-impose Liouville-like behavior on the demon, then we are simply building the second law into the demon by fiat, rather than deriving it.

This is precisely what several philosophers of physics have criticized as *circular* in much of the Landauer-based Maxwell-demon literature. Hemmo and Shenker [39], for example, argue that when Landauer's principle is grounded in the second law ("the entropy of a closed system cannot decrease"), and then used in turn to *defend* the universality of the second law against Maxwell's demon, "grounding its proof in the second law is viciously circular" [40]. Norton and Maroney likewise emphasize that many exorcisms simply assume some hidden entropy production must exist in the demon, lest the second law be violated, and then present this as proof that the demon cannot work [41] [42].

Seen from this angle, the standard information-theoretic exorcisms are *conditional* statements: *if* all microscopic dynamics (including the demon's internal channel) are time-reversal symmetric and Liouvillean, and *if* one adopts the usual second-law constraint for closed systems, *then* any demon must pay back at least as much entropy as it removes. They do not address, and cannot rule out, demons whose essential operation relies on a genuinely *time-reversal-asymmetric* physical process. In other words, when these exorcisms are invoked to claim that *no* demon can ever reduce total entropy, their use becomes circular: they presuppose the very form of the second law (and the underlying symmetry assumptions) that is under scrutiny.

6.2. Not All Laws of Nature Are Time-Reversal Symmetric

In this context, it is also important to recall that *not all physical laws are time-reversal symmetric, even at the classical level.* Electromagnetism in particular, admits phenomena whose operational behavior is *manifestly asymmetric* under time-reversal when treated in their effective (non-Hamiltonian) forms. Examples

include the well-known $E\times B$ drift in plasmas and the $E\times B$ thermoelectric effect by Levy [2]-[6] in semiconductors cited earlier in this paper. In such systems, the cross-field drift velocity:

$$\boldsymbol{v}_{E\times B} = \frac{\boldsymbol{E}\times\boldsymbol{B}}{B^2} \tag{62}$$

does not reverse sign under the naive time-reversal operation unless one also changes the sign of the magnetic field.

Levy [7] presents a thought experiment aimed at testing time-reversal symmetry: a charged particle moves through a magnetic field $\boldsymbol{B}$. Under time reversal, velocities reverse sign, $\boldsymbol{v}\to-\boldsymbol{v}$, but the magnetic field, being generated by currents external to the experiment, does not automatically reverse. causing the Lorentz force $q\boldsymbol{v}\times\boldsymbol{B}$ to change sign.

This creates a dilemma. If we time-reverse only the particle (keeping the external field fixed), the particle's trajectory does not retrace itself—it curves the opposite way—the particle subsystem is therefore intrinsically time-asymmetric revealing a microscopic arrow of time. If instead, we include the field source mechanism in the time-reversed system, then $\boldsymbol{B}$ flips sign along with the particle's velocity, but **now the entire experimental apparatus is time-reversal asymmetric,** and we are no longer performing the same experiment in reverse. Either way, the magnetic field introduces an irreducible time asymmetry: the system cannot be returned to its initial state by time reversal alone.

Physical channels with genuine dynamical time asymmetry are well known in plasma physics, thermoelectricity, and magnetotransport. As shown by Aguilar *et al.* [43], quantum mechanical effects can also produce time asymmetry. A demon operating through such a channel is *not* constrained by the symmetric-Liouville assumptions underlying the Brillouin-Landauer-Bennett program, and therefore its entropy accounting requires a fresh analysis, such as the $\Delta S_A + \Delta S_B$ decomposition developed here.

In summary, Nature is not universally time-reversal symmetric, yet as discussed above, conventional thermodynamics uniformly assumes this symmetry in:

- All H-theorems by Boltzmann [19]-[21], Tolman [22], Gibbs [23], Von Neumann [24].
- All fluctuation theorems by Evans, Cohen, and Morriss [26], Evans, D. J Searles [27] [28], and G. E. Crooks [29].
- All exorcisms of Maxwell's demon by Brillouin [34] [35], Landauer [36], and Bennett [37] [38].
- Reciprocals by Onsager [1].

6.3. Including Time-Reversal in Thermodynamics

The present proposal should therefore be understood as exploring precisely the regime that the H-Theorems and the Brillouin-Landauer-Bennett framework does not cover: physical systems in which a nonzero time-asymmetric contribution $\Delta S_B < 0$ rises from *intrinsically time-reversal-asymmetric microscopic dynamics.* In

this regime, Liouville-volume preservation and the associated Landauer-style entropy inequalities do not apply by default; they must be re-derived from the actual dynamics rather than imported as axioms. The bound proposed in Equation (60),

$$W \le \frac{\Delta G_B}{2} = -\frac{T\Delta S_B}{2} \tag{63}$$

should therefore be viewed not as an extension of the Landauer bound, but as its *replacement* in the presence of genuine dynamical time-asymmetry. It characterizes the maximum extractable work from a process whose irreversibility originates not in logical erasure or coarse-graining, but in the fundamental directionality of the underlying physical interaction. This stands in clear contrast to the Brillouin-Landauer-Bennett analyses, which apply only when the demon's internal channel obeys microscopic time-reversal symmetry and Liouville's theorem, *i.e.*, when $\Delta S_B = 0$.

6.4. Information Theoretic Interpretation

The concept of bandwidth discussed herein is directly analogous to *Rolf Landauer's channel bandwidth concept*, but applies to a *physical*, *thermodynamic channel* rather than a purely computational one. Specifically, the demon-trapdoor-turbine system is treated as an information processing channel having a maximum speed determined by the reaction time of the demon and the combined mean free time of N gas molecules (*i.e.*, $\tau_{MeanFreeTime}/N$). The key result is that optimal operation requires *matching the demon's bandwidth to the thermal fluctuation bandwidth* of the gas; otherwise, information (negentropy) is either wasted or drowned in noise.

Just as in Landauer's framework, a communication or computation channel has a finite capacity that limits how fast information can be processed reliably. The *minimum dissipation per bit erased* formulated by Landauer, is mirrored with *a maximum extractable power* in this paper. Under optimal conditions, *only half of the demon's available bandwidth* (*and free energy production rate*) *can be delivered to the load*, with the remainder necessarily dissipated in symmetric processes.

This paper diverges critically from Landauer in two respects:

1) Energy and bandwidth are treated as conjugate quantities, both having thermodynamic meaning, and both scaling identically with heat and flux. This key insight extends Landauer's framework by treating bandwidth *not just as a system constraint but as an optimizable parameter generated by a heat source*—**gas particles carrying thermal energy have a bandwidth.**

2) Information channels can be time-asymmetric. Landauer's analysis assumes time-reversal symmetric dynamics (Liouvillean evolution), which leads to his minimum dissipation bound. This paper explicitly considers time-asymmetric channels where this bound may not apply—the demon's bandwidth is not constrained by Landauer's erasure cost because the asymmetric dynamics generate negentropy directly at a rate proportional to the asymmetry.

In short, the Landauer's channel-capacity idea is reframed as a *thermodynamic*

bandwidth-matching constraint that governs how much negentropy per unit time can be generated and converted into useful power in *a time-asymmetric physical system*.

6.5. Geometric Interpretation of Data Channels

The paper treats information channels as geometric physical apertures which have bandwidths that scale with meters, not just bits—showing that optimal thermodynamic information processing emerges only when spatial dimensions (mean free path, cross-sectional area, chamber size) are precisely matched to the time and energy scales of thermal motion as shown in Equation (49):

$$A_{Door} = A_{Turbine} = 2A_{Source} = 2A_{Load} \tag{64}$$

The demon acquires information about particles and processes them as they cross a surface (the trapdoor). Therefore, information processing is fundamentally a surface phenomenon that scales with *area*, not volume. This dimensional dependency suggests that any practical implementation should maximize the surface area of the time-asymmetric interface relative to the working volume.

6.6. Connection with the Holographic Principle

The area-scaling of information bandwidth in this analysis invites comparison with the holographic principle in gravitational physics, where the maximum entropy of a bounded region scales with its surface area rather than its volume. The Bekenstein-Hawking formula $S = A/(2L_P)^2$ (where S is entropy, A is the horizon's surface area and L_P is Planck's length) establishes that black hole entropy is proportional to horizon area, a result that 't Hooft and Susskind generalized into the holographic principle: the information content of any spatial region is determined by its boundary area in Planck units.

The Bekenstein-Hawking formula suggests a horizon's surface A divided into information "pixels" of size $2L_P$. The entropy S_{BH} of a black hole would then be equal to the number of pixels $A/(2L_P)^2$. This viewpoint is highly remindful of the architecture presented in **Figure 6**, in which an array of demons forms a surface, each demon operating as an independent agent on a single gas particle.

However, the parallel should be stated carefully. The holographic principle constrains the *total information content* of a spatial region, whereas the present result concerns the *rate of information flow*—(*i.e.*, bandwidth) which scales with area because the demon acquires information at a two-dimensional interface where particles cross a decision boundary. Despite this distinction, both results share a common geometry: fundamental information-theoretic quantities are surface-limited rather than volume-limited. In kinetic theory, this emerges because particle flux is intrinsically a surface-crossing quantity.

In this light, standard derivations of black hole entropy appear incomplete because they rely on time-reversal symmetric dynamics and equilibrium thermodynamics. In fact, astrophysical black holes are rarely symmetric: rotation produces frame-dragging in the ergosphere, accretion disks generate strong magnetic fields,

and charge separation can occur in the surrounding plasma. These features introduce time-asymmetries analogous to those exploited by the demon.

Consider the Penrose process, which extracts energy from a rotating black hole's ergosphere. This is conventionally framed as tapping rotational energy, but the underlying mechanism relies on frame-dragging creating a preferred temporal direction-particles in the ergosphere experience an environment that is manifestly not time-symmetric. Similarly, magnetic fields near the horizon would induce $E\times B$ drifts in charged particles, another time-asymmetric phenomenon.

This raises several open questions:

1) Does the standard black hole entropy require modification in the presence of strong time-asymmetric processes such as rotation or magnetic fields near the horizon?

2) Can the framework developed in this paper, which explicitly distinguishes time-symmetric (ΔS_A) and time-asymmetric (ΔS_B) entropy contributions, be extended to horizons and other gravitational boundaries?

3) Is the Penrose process an instance of time-asymmetric negentropy generation analogous to the demon's operation, rather than mere energy extraction?

4) More generally, when a system's information-theoretic results are derived assuming time-reversal symmetry, how must those results be revised for systems with intrinsic temporal asymmetry?

These questions suggest that the intersection of time-reversal asymmetry, information theory, and gravitational thermodynamics may be a fruitful area for future investigation. The tools developed here for mesoscopic systems-particularly the partitioning of entropy into symmetric and asymmetric components and the optimization of bandwidth as a conjugate variable to energy—may offer a starting point for such inquiries.

7. Conclusions

This paper uses Szilard's pressure demon, a variation of Maxwell's demon, as a proxy for the analysis and optimization of anomalous thermodynamic phenomena caused by time-reversal asymmetry. These phenomena are responsible for the $E\times B$ thermoelectric effect [2]-[6], diode rectification of the Johnson-Nyquist noise [8], anomalous thermodynamics in biological organisms [9]-[11], asymmetric membranes [12] [14] and anomalous superconductive effect [16] [17].

Time-reversal asymmetric systems are not bound by the H-theorem. Experimental data showing anomalous behavior does exist, but it is scant. To be observable such experiments must incorporate two essential requirements:

1) A time-reversal asymmetric phenomenon as manifested, for example by a magnetic field or a diode.

2) Matching an asymmetry measure to a corresponding time-reversal symmetry measure of the surrounding thermal processes. For example, the current voltage "knee" of the diode should be commensurate with the thermal fluctuations—e.g., the Johnson-Nyquist noise—to be rectified. Without proper match-

ing, anomalous thermodynamic behavior remains too small to be observable.

The first requirement eliminates H-theorems as theoretical obstacles to achieving anomalous results. The second, eliminates the large body of negative experimental results because of their failure to include the stringent symmetry/asymmetry matching condition.

Therefore, the task of producing useful energy from ambient heat morphs from a theoretical impossibility to the engineering task of finding the right materials and design. The second law can be bypassed without violating any physical law.

This paper provides a "roadmap" that relies on the thermodynamic threshold optimization to design devices based on time-reversal asymmetric phenomena such as the $E \times B$ drift, MIM diodes, and asymmetric membranes. This method uses the first and second laws as constraints, and energy and bandwidth outputs as optimization criteria. The optimization method is a thermal analog of electrical source-load matching that maximizes power transfer from source to load.

A fully optimized Szilard's demon acting on air molecules at STP can produce a power per unit area of 1276 mW/mm^2, or about 1000 times the solar irradiance of 1.33 mW/mm^2, and a power per unit volume of 74.1 KW/mm^3. This enormous power is due to the massive parallelism of multiple demons operating in parallel, each one in a chamber 17 nm on the side, and each chamber holding a single particle. Obviously, without replacing the thermal energy converted to work, such output cannot be maintained for more than approximately the mean free time of a particle. The small dimensions of this design may be achievable on semiconductors in which electrical carriers replace gas particles.

In analogy to the Maximum Power Transfer Theorem in electrical engineering, the second law is extended to limit the power output of time-reversal asymmetric systems to half the free energy they produce per second. In a Goldilocks fashion, the rest of the free energy is spent in frictional processes such as particle collisions which are detrimental because they slow down heat to work conversion, yet necessary to enable heat flow and replenish the converted thermal energy.

Acknowledgements

I thank my wife Penny for her unwavering support, and my children, grandchildren and all future generations of the world who motivate me to pursue this research for tikkun olam.

Data Availability Statement

Please contact the author for additional information.

Conflicts of Interest

The author declares no conflict of interest.

References

[1] Levy, G.S. (2019) Loschmidt's Paradox, Extended to CPT Symmetry, Bypasses Sec-

ond Law. *Journal of Applied Mathematics and Physics*, **7**, 3140-3175. https://doi.org/10.4236/jamp.2019.712221

[2] Levy, G.S. (2023) An Overview of the ExB Thermoelectric Effect. *MRS Advances*, **8**, 113-118. https://doi.org/10.1557/s43580-023-00521-5

[3] Levy, G.S. (2022) The ExB Thermoelectric Effect. https://youtu.be/CBenek-3MGs

[4] Levy, G.S. (2023) The ExB Thermoelectric Effect Bypasses the Second Law. ResearchGate. https://doi.org/10.13140/RG.2.2.29199.56483

[5] Levy, G.S. (2020) ExB Drift Thermoelectric Energy Generation Device. US Patent 10971669.

[6] Levy, G.S. (2024) ExB Drift Thermoelectric Energy Device. PCT Patent Application No.: PCT/US2024/024668.

[7] Levy, G.S. (2025) Isothermal Magnetostrictive Convection. *Journal of Applied Mathematics and Physics*, **13**, 3352-3392. https://doi.org/10.4236/jamp.2025.1310193

[8] Kondo, S., Kameyama, M., Imaoka, K., Shimoi, Y., Mathevet, F., Fujihara, T., *et al.* (2024) Organic Thermoelectric Device Utilizing Charge Transfer Interface as the Charge Generation by Harvesting Thermal Energy. *Nature Communications*, **15**, Article No. 8115. https://doi.org/10.1038/s41467-024-52047-5

[9] Lee, J.W. (2024) Type-B Energetic Processes: Their Identification and Implications. *Symmetry*, **16**, Article 808. https://doi.org/10.3390/sym16070808

[10] Lee, J.W. (2022) Type-B Energy Process: Asymmetric Function-Gated Isothermal Electricity Production. *Energies*, **15**, Article 7020. https://doi.org/10.3390/en15197020

[11] Lee, J.W. (2022) Type-B Energetic Processes and Their Associated Scientific Implications. *Journal of Scientific Exploration*, **36**, 484-492. https://doi.org/10.31275/20222517

[12] Sheehan, D.P. (2023) A Self-Charging Concentration Cell: Theory. *Batteries*, **9**, Article 372. https://doi.org/10.3390/batteries9070372

[13] Sheehan, D.P., Hebert, M.R. and Keogh, D.M. (2022) Concentration Cell Powered by a Chemically Asymmetric Membrane: Experiment. *Sustainable Energy Technologies and Assessments*, **52**, Article ID: 102194. https://doi.org/10.1016/j.seta.2022.102194

[14] Sheehan, D.P., Watson, A.J., Welsh, T.M., Gibson, C.C., Miller, D.W. and Glick, J. (2023) Numerical Simulations of Diffusion-Driven Concentration Gradients in Chemically Asymmetric Membranes: Implications for Sustainable Energy and the Second Law of Thermodynamics.

[15] Sheehan, D.P., Garamella, J.T., Mallin, D.J. and Sheehan, W.F. (2012) Steady-State Nonequilibrium Temperature Gradients in Hydrogen Gas-Metal Systems: Challenging the Second Law of Thermodynamics. *Physica Scripta*, **151**, Article ID: 014030. https://doi.org/10.1088/0031-8949/2012/t151/014030

[16] Nikulov, A.V. (2021) Dynamic Processes in Superconductors and the Laws of Thermodynamics. *Physica C: Superconductivity and Its Applications*, **589**, Article ID: 1353934. https://doi.org/10.1016/j.physc.2021.1353934

[17] Gurtovoi, V.L., Antonov, V.N., Exarchos, M., Il'in, A.I. and Nikulov, A.V. (2019) The Dc Power Observed on the Half of Asymmetric Superconducting Ring in Which Current Flows against Electric Field. *Physica C: Superconductivity and its Applications*, **559**, 14-20. https://doi.org/10.1016/j.physc.2019.01.009

[18] Fu, X. and Fu, Z. (2003) Realization of Maxwell's Hypothesis: A Heat-Electric Conversion in Contradiction to the Kelvin Statement. arXiv: physics/0311104.

[19] Boltzmann, L. (1872). Weitere studien über das wärmegleichgewicht unter gasmolekülen. In: Boltzmann, L., Eds., *Kinetische Theorie II*, Vieweg + Teubner Verlag, 115-225. English Translation "Further Studies on the Thermal Equilibrium of Gas Molecules" in S. G. Brush's Kinetic Theory, Vol. 2: Irreversible Processes (Published in 2003 by Elsevier/Pergamon).

[20] Parker, S.P. (1993) Encyclopedia of Physics. 2nd Edition, McGraw Hill.

[21] Chapman, S. (1937) Boltzmann's H-Theorem. *Nature*, **139**, 931-931. https://doi.org/10.1038/139931a0

[22] Tolman, R.C. (1938) The Principle of Statistical Mechanics. The Clarendon Press, 138 p. https://archive.org/details/ThePrinciplesOfStatisticalMechanicsTolmanOxfordAtTheClarendonPress1938

[23] Gibbs, J.W. (1902) Elementary Principles in Statistical Mechanics Developed with Especial Reference to the Rational Foundation of Thermodynamics. Charles Scribner's Sons. https://doi.org/10.5962/bhl.title.32624

[24] von Neumann, J. (2010) Proof of the Ergodic Theorem and the H-Theorem in Quantum Mechanics. *The European Physical Journal H*, **35**, 201-237. https://doi.org/10.1140/epjh/e2010-00008-5

[25] Von Neumann, J. (1955) Mathematical Foundations of Quantum Mechanics. Princeton University Press.

[26] Evans, D.J., Cohen, E.G.D. and Morriss, G.P. (1993) Probability of Second Law Violation in Shearing Steady States. *Physical Review Letters*, **71**, 2401-2404. https://pdfs.semanticscholar.org/697a/31eace27d3b0096700709d83d5f3bd8f1733.pdf

[27] Evans, D.J. and Searles, D.J. (1996) Causality, Response Theory, and the Second Law of Thermodynamics. *Physical Review E*, **53**, 5808-5815. https://doi.org/10.1103/physreve.53.5808

[28] Evans, D.J. and Searles, D.J. (2002) The Fluctuation Theorem. *Advances in Physics*, **51**, 1529-1585. https://pdfs.semanticscholar.org/470a/4e148c2ba7aa0f6d48d455d9a854db2a1da2.pdf

[29] Crooks, G.E. (1999) Entropy Production Fluctuation Theorem and the Nonequilibrium Work Relation for Free Energy Differences. *Physical Review E*, **60**, 2721-2726. https://doi.org/10.1103/physreve.60.2721

[30] Rex, A. (2017) Maxwell's Demon—A Historical Review. *Entropy*, **19**, Article 240. https://doi.org/10.3390/e19060240

[31] Szilard, L. (1929) Über die Entropieverminderung in einem thermodynamischen System bei Eingriffen intelligenter Wesen. *Zeitschrift für Physik*, **53**, 840-856. https://doi.org/10.1007/bf01341281

[32] NASA: Solar Irradiance. https://earth.gsfc.nasa.gov/climate/projects/solar-irradiance

[33] Shockley, W. and Queisser, H.J. (1961) Detailed Balance Limit of Efficiency of *P-N* Junction Solar Cells. *Journal of Applied Physics*, **32**, 510-519. https://doi.org/10.1063/1.1736034

[34] Brillouin, L. (1951) Maxwell's Demon Cannot Operate: Information and Entropy. I. *Journal of Applied Physics*, **22**, 334-337. https://doi.org/10.1063/1.1699951

[35] Brillouin, L. (1962) Science and Information Theory. 2nd Edition, Academic Press. https://books.google.com/books/about/Science_and_Information_Theory.html?id=tPXVbiw_1P0C&utm_source=chatgpt.com

[36] Landauer, R. (1961) Irreversibility and Heat Generation in the Computing Process. *IBM Journal of Research and Development*, **5**, 183-191. https://doi.org/10.1147/rd.53.0183

[37] Bennett, C.H. (1973) Logical Reversibility of Computation. *IBM Journal of Research and Development*, **17**, 525-532. https://doi.org/10.1147/rd.176.0525

[38] Bennett, C.H. (2003) Notes on Landauer's Principle, Reversible Computation, and Maxwell's Demon. *Studies in History and Philosophy of Science Part B: Studies in History and Philosophy of Modern Physics*, **34**, 501-510. https://doi.org/10.1016/s1355-2198(03)00039-x

[39] Hemmo, M. and Shenker, O. (2019) The Physics of Implementing Logic: Landauer's Principle and the Multiple-Computations Theorem. *Studies in History and Philosophy of Science Part B: Studies in History and Philosophy of Modern Physics*, **68**, 90-105. https://doi.org/10.1016/j.shpsb.2019.07.001

[40] Shenker, O. and Hemmo, M. (2020) Maxwell's Demon in Quantum Mechanics. *Entropy*, **22**, Article 269. https://doi.org/10.3390/e22030269

[41] Norton, J.D. (2005) Eaters of the Lotus: Landauer's Principle and the Return of Maxwell's Demon. *Studies in History and Philosophy of Science Part B: Studies in History and Philosophy of Modern Physics*, **36**, 375-411. https://doi.org/10.1016/j.shpsb.2004.12.002

[42] Maroney, O.J.E. (2009) Information Processing and Thermodynamic Entropy. Stanford Encyclopedia of Philosophy.

[43] Aguilar, M. and Lutz, E. (2025) Correlated Quantum Machines Beyond the Standard Second Law. *Science Advances*, **11**, eadw8462. https://doi.org/10.1126/sciadv.adw8462

Appendix 1. List of Symbols

A	Cross-sectional area
d	Diameter of a particle
G	Free energy
k_B	Boltzmann's constant
m	Mass of a particle
N	Number of gas particles
n_1	Particle concentration upstream of demon and downstream of turbine
n_2	Particle concentration downstream of demon and upstream of turbine
P	Power
p_1	Pressure upstream of demon and downstream of turbine
p_2	Pressure downstream of demon and upstream of turbine
Q	Heat drawn from heat bath
S	Entropy
T	Temperature of gas
T_0	Temperature of heat bath
U	Internal energy
v	Axial velocity along a single degree of freedom
V	Volume of gas
W	Work performed by turbine
α	$p_2/p_1 = n_2/n_1$
β	Bandwidth
δ_{Res}	Optical resolution of demon
$\delta_{xChamber}$, $\delta_{yChamber}$, $\delta_{zChamber}$	Dimensions of chamber
λ	Mean free path
τ_{Demon}	Demon's reaction time
$\tau_{MeanFreeTime}$	Mean-free-time

Appendix 2. Thermodynamic Cycle of the Demon

The demon follows a thermodynamic cycle illustrated in Figure A1(a) and Figure A1(b), comprised of two stages.

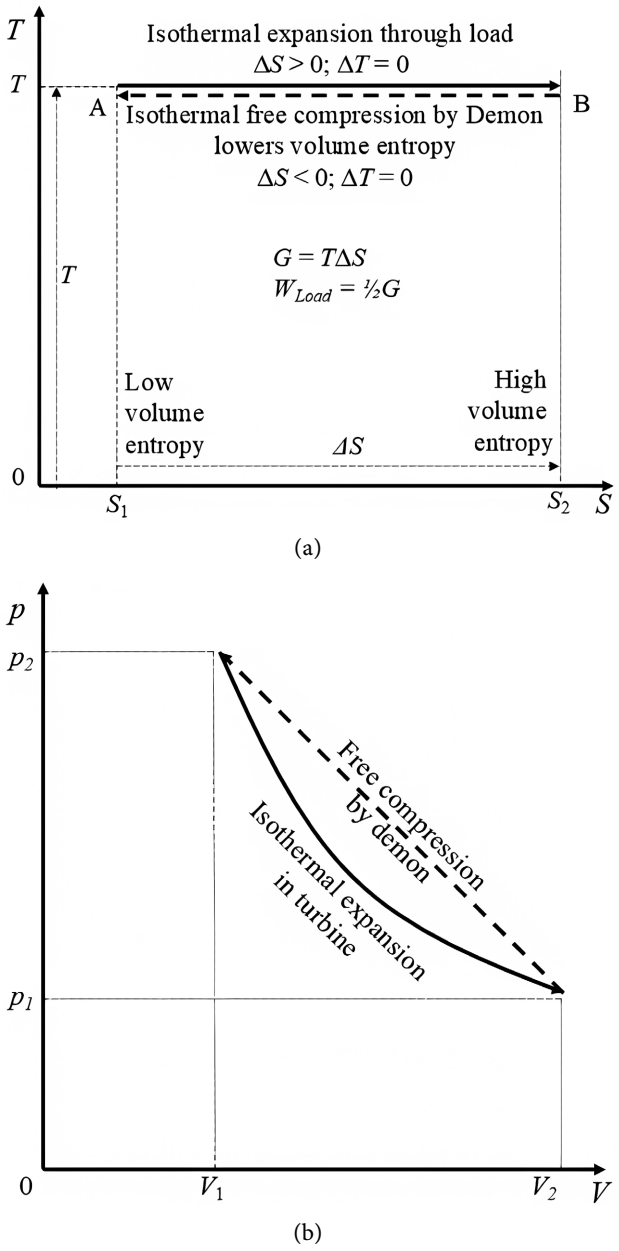

Figure A1. Thermodynamic cycle: (a) temperature entropy diagram; (b), pressure volume diagram.

1) Stage 1 is a compression of the gas from the left compartment to the right one, caused by the action of the demon and trapdoor on the gas. Since the door is perfectly elastic when closed and transmissive when open, it does not alter the internal energy of interacting particles. Therefore, the compression of the gas is isothermal and adiabatic. In effect it is a "free compression" in analogy to the well-known "free expansion".

2) Stage 2 is an isothermal expansion of the gas through the turbine which extracts heat from the surroundings and produces work. For the purposes of analytical clarity, the operation of the turbine is split in two:

a) An adiabatic frictionless expansion which utilizes the free energy (in the form of a pressure difference) from the demon to convert heat to work.

b) An isochoric heat transfer from the surroundings which replenishes the heat converted to work.

Both of these functions operate in tandem, and incrementally with each other. In combin ation, the adiabatic expansion and isochoric heat transfer are isothermal. **Figure A1(a)** is a temperature-entropy diagram which shows that the free energy produced by the demon is $T\Delta S$. Optimally, half of this free energy is converted to work by the turbine, and the other half is used up by friction in the heat source which operates as a heat exchanger with the surrounding heat bath.